Neutrino Detection with the Surface Array of the Pierre Auger Observatory

A. Tamburro[a§] for the Pierre Auger Collaboration[b]
[a]Institut für Experimentelle Kernphysik Universität Karlsruhe, Germany
[b]Observatorio Pierre Auger, Av. San Martin Norte, 5613 Malargüe, Argentinia
[§] corresponding author, Email: alessio.tamburro@ik.fzk.de
Telephone: +49-7247-82-4978, Fax: +49-7247-82 4075

***Abstract*— The Pierre Auger Observatory has the capability of detecting neutrino-induced extensive air showers by searching for very inclined showers with a significant electromagnetic component. In order to study the detector response of the surface array of the Pierre Auger Observatory, Monte Carlo simulations of up-going and down-going neutrino showers for all flavors were performed. A set of relevant observables were determined to discriminate these showers from the background of very inclined hadronic showers and the identification efficiency was studied. The acceptance and the expected event rates, based on the assumption of the incoming neutrino flux, were finally calculated.**

I. Introduction

Searching for high-energy neutrinos ($10^{18}\,\mathrm{eV}$ or above) emitted from astrophysical objects is one of the most challenging field in Astroparticle Physics. Neutrinos offer a unique opportunity to open a new observation window, since they are only weakly interacting and neutral [1]. After having traveled cosmological distances without being perturbed and/or deflected in the interstellar medium, neutrinos behaves as messengers of the most mysterious regions of astrophysical sources.

Astrophysical neutrinos of any flavor, ν_l, are expected to be observed by detecting the leptons, l, induced with Deep Inelastic Scattering (DIS) processes on nuclei, N, of the traversed matter, in the charged current (CC) interaction channel or in the neutral current (NC) interaction channel, according to the following reaction:

$$[CC] \quad \nu_l + N \rightarrow l + X, \tag{1}$$

$$[NC] \quad \nu_l + N \rightarrow \nu_l + X, \tag{2}$$

where X represents the outgoing fragments of hadrons. Neutrinos with energy E_ν such that $10^{16} < E_\nu < 10^{21}\,\mathrm{eV}$ are predicted to have cross-sections which increase typically as $E_\nu^{1/3}$ [2]. The cross-section for NC ν-nucleon interaction is expected to be 1/3 smaller than the cross-section for CC interactions. Nevertheless, at the highest energies (or low Bjorken-x, $x \lesssim 10^{-5}$), extrapolation of the cross-section is needed [3]. The more conventional cross-sections termed as GRV98lo [4] will be considered in this work.

Several theoretical models predict a significant flux of high-energy neutrinos associated to the emission of a flux of particles (see e.g. [5]), generally called cosmic rays, at macroscopic energies of about $10^{18}\,\mathrm{eV}$ or larger along with gamma rays (*beam dump* scenario). The emerging ν flux, $\phi_{\nu_l} = dN/dE_{\nu_l}$, is distributed among the flavors according to $\phi_{\nu_e} : \phi_{\nu_\mu} : \phi_{\nu_\tau} = 1 : 2 : 0$ for a large range of different spectra of parent particles. Neutrino oscillations, confirmed by atmospheric and solar neutrino data [6, 7], modify the expected flavor ratio during the propagation from the sources to the observation point [8, 9] to $\phi_{\nu_e} : \phi_{\nu_\mu} : \phi_{\nu_\tau} = 1 : 1 : 1$. Exotic phenomena can modify even drastically this scenario [10, 11, 12].

An additional challenging observational window for neutrinos is from propagation of ultra-high energy cosmic rays in the interstellar medium (GZK neutrinos [13]). In this scenario, ν is expected to be produced by the interaction of primary cosmic rays with the cosmic microwave background through inverse photoproduction of a Δ^+ resonance.

Extensive air showers (EAS) which are initiated by the interaction of primary cosmic rays in the atmosphere, are continuosly detected on the ground by large arrays of detectors, which sample their lateral distribution, and/or fluorescence detectors, which reveal the ultraviolet radiation emitted by the excitation of nitrogen during the passage of particles in the atmosphere. The Pierre Auger Observatory [14] synthetizes the two detection techniques in a hybrid technique and offers the possibility to improve event reconstruction quality and reduce systematic errors.

One of the observations, made possible by the observatory, is the detection of high-energy neutrinos [15, 16, 17, 18] and a limit was put by the Pierre Auger Collaboration in case of up-going ν_τ [19]. At large zenith angles ($\theta \gtrsim 70°$) ν showers may be distinguished from hadronic showers by searching for the typical features of *young* showers (shower maximum close to the ground) as well as of elongated and asymmetric footprints. The background to neutrino detection is mainly due to proton-induced showers, which are able to survive to the ground as *old* showers (shower maximum far from the ground). The surface array of the observatory consists of an array of water Cherenkov detectors which can differentiate signals produced by muons from signals produced by electrons and, thus, to discriminate between young and old showers. Down-going ν_τ and ν_e, and up-going ν_τ are expected to be revealed in the huge background of detected hadronic cosmic rays [20, 21, 22, 23]. Up-going ν_τ have a chance to induce detectable EAS only if their incoming direction ranges up to few degrees below the horizon [24, 25], scratching the Earth's crust (Earth-skimming ν). The surrounding Andes mountains enhance the sensitivity of the observatory to τ-induced showers [26, 25, 19]. Not only do the expected neutrino detection rates depend on the incoming flux, but also the ν-nucleon cross-section and the τ energy loss at the highest energies give rise to important contributions to the systematic uncertainty of calculated rates [27].

In this work a study on detecting high-energy neutrinos with the surface array of the Pierre Auger Observatory will be presented. After a short description of the performances of the surface detector array (Sec. II), the Monte Carlo (MC) chain implemented to simulate ν-induced showers will be discussed (Sec. III). Simulations are needed to study the signatures expected from ν-induced showers and to define suitable observables which allow their identification (Sec. IV). Finally, sensitivity and expected event rates will be given (Sec. V). An outlook to the upcoming future shows that further studies to improve the present work can be forseen (Sec. VI).

II. THE SURFACE DETECTOR ARRAY OF THE OBSERVATORY

The Pierre Auger Observatory [14], located near Malargue in the province of Mendoza, Argentina, is being built as a hybrid-detector. It combines the measurement of the particles at the ground – by means of a huge array of water Cherenkov detectors – with the measurement of the fluorescence light produced by EAS in the atmosphere. The surface detector array (SD) consists of about 1600 water Cherenkov detectors (tanks) arranged in a triangular grid with 1.5 km spacing. Each Cherenkov detector consists of three photomultipliers (PMTs) on the top, which samples the shower signal with a 40 MHz flash analog-to-digital converter (FADC). A Tyvek coverage of the internal wall of each station guarantees a complete diffusion of the Cherenkov light. At each station of the surface detector, the FADCs sample the current generated at the PMTs and return a measure of the light produced by particles crossing the water Cherenkov station. The signal detected at each station refers to a common calibration unit, the so-called vertical equivalent muon or VEM [28]. Two separate local hardware triggers are implemented at each station. They form the first level trigger and are a simple threshold trigger and a time-over-threshold trigger (ToT). In particular, the nominal ToT trigger requires the signal to be above $0.2\,\mathrm{VEM}$ in at least 2 PMTs for a minimum of 13 bins ($325\,\mathrm{ns}$) within a sliding time window of 120 time bins ($3\,\mu\mathrm{s}$). The ToT trigger was designed to detect broader signals and, thus, it is suitable to identify signals produced by the electromagnetic component of showers. The threshold trigger requires the signal to be above $1.75\,\mathrm{VEM}$ in at least 1 PMTs for $25\,\mathrm{ns}$ and was designed to detect fast signals, typically produced by the muonic component of showers. A second level trigger selects multiplet of first level triggers and, finally, a third level trigger may accept a multiplet as possible physical shower on the basis of space-time coincidences.

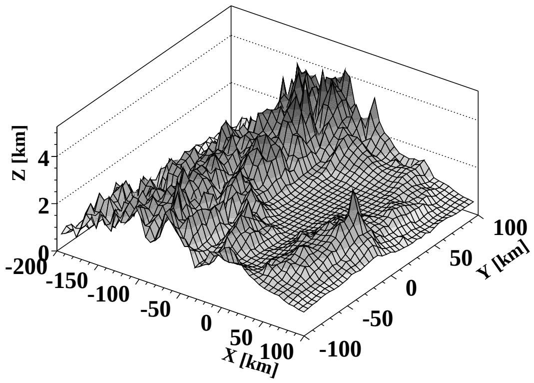

Fig. 1. *Topography of the Southern site according to CGIAR-CSI data. The center of the map corresponds to the center of the Auger array (latitude $\phi_{SO} = 35.25°$ S, longitude $\lambda_{Auger\,center} = 69.25°$ W). The Auger position can be approximately localized in the center of the flat area.*

In order to retain all the detector performances, a framework, called $\overline{\text{Off}}\underline{\text{line}}$ [29], was designed to simulate and reconstruct EAS.

III. SIMULATING ν-INDUCED AND PROTON-INDUCED SHOWERS

In order to study the signatures expected from ν-induced showers at the surface array of the observatory, a full MC simulation chain was set. Simulation of neutrino signatures consists of three phases: propagation and interaction inside the earth and atmosphere to produce primaries able to initiate potentially detectable showers in the atmosphere; simulation of lateral profiles of shower developments in the atmosphere and, finally, simulation of detector response.

The initial incoming ν-flux is propagated through the encountered matter (Earth, its atmosphere or both), until an interaction takes place by using an extended version of the code ANIS [26]. First, for fixed neutrino energies, 10^6 events were generated with zenith angles in the range $[60°, 90°]$ (down-going showers) and $[90°, 95°]$ (up-going showers) and with azimuth angles in the range $[0°, 360°]$ on the top of the atmosphere. Then, neutrinos were propagated along their trajectories of length ΔL from the generation point to the backside of the detector array in steps of $\Delta L/1000$ ($\geq 6\,\mathrm{km}$). At each step of propagation, the ν–nucleon interaction probability was calculated according to the parameterization of the cross-section GRV98lo [4]. The propagation of τ leptons through the Earth was simulated by using the energy loss model of Ref. [30]. Electrons, instead, were assumed to interact immediately with the surrounding medium. If the interaction takes place in the atmosphere, an EAS is, thus, produced. All the computations were done by using digital elevation maps (DEM, Fig. 1) [31] and, then, they were repeated by using the spherical model of the Earth (SP), with its radius set to $6371\,\mathrm{km}$ (sea level). The flux of outcoming leptons as well as their energy and decay vertex position were calculated inside a defined detector volume. The geometrical size of the volume was set to $50 \times 60 \times 10\,\mathrm{km}^3$ and it included the real shape

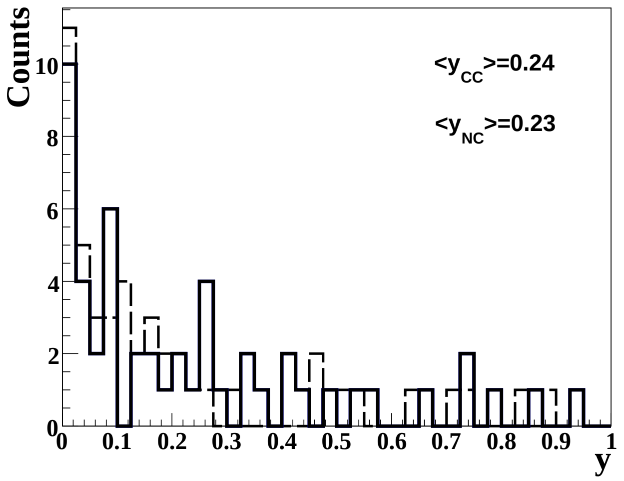

Fig. 2. *The inelascticity distribution in CC (solid line) and NC (dashed line) interactions of 50 simulated ν events at $E_\nu = 10^{18}\,\mathrm{eV}$, as obtained from PYTHIA.*

of the Auger Observatory on the ground at its completion. The detector was positioned at $1430\,\mathrm{m}$ above sea level, which corresponds approximately to the average altitude of the array. In case of computations with the simple spherical model of the Earth, the same size of the detector volume was assumed, but the detector position was set at $10\,\mathrm{m}$ above the sea level. The additional outcoming particle spectrum from deep inelastic NC and CC ν-nucleon interactions was simulated by using the event generator PYTHIA [32]. In Fig. 2 the distribution of the inelasticity[1] of ν_e CC and NC interactions is shown. Both the distributions show a similar behaviour and the average values agree quite well with the canonical value of 0.2. In case of ν_e CC interactions, the outcoming electrons are expected to induce electromagnetic showers at the same point where the hadronic products induce hadronic showers. In case of ν_τ CC interactions, the produced τ leptons can travel some distance in the atmosphere and decay into particles which can induce a detectable shower. Thus, outcoming hadronic showers initiated by ν_τ are usually separated by a certain distance from showers initiated by tau decay products. In this particular case, tau decays were simulated by using the additional package TAUOLA [33]. Finally, muons produced in ν_μ CC interactions are expected to induce showers which are generally weaker, with a smaller energy transfer to EAS, and, thus, with a suppressed longitudinal profile and much fewer particles on the ground. The detection probability is expected to be strongly reduced. Interactions in the NC channel induce only pure hadronic showers whose primaries are generated with PYTHIA.

Lateral profiles (particle density distributions of secondaries) of shower developments were generated by using PYTHIA and/or TAUOLA output as input for the EAS MC generator AIRES [34]. A special mode was used to inject simultaneously several particles or primaries (namely, the products of ν-nucleon interactions) at a given interaction point. Showers induced by the products of up-going decaying τ leptons with energies from $0.1\,\mathrm{EeV}$ to $100\,\mathrm{EeV}$ at altitudes of decay points from 0 to $3500\,\mathrm{m}$ above the ground level, with step $100\,\mathrm{m}$, were simulated. At each altitude 40 events were generated to cover the tau decay channels implemented in ANIS. In case of down-going showers, the decay altitudes were distributed from the ground level up to the altitude corresponding to the beginning of the atmosphere for fixed zenith angle. For example, for down-going electrons, the particles produced by PYTHIA were inserted at different slant depths measured from the ground up to $3000\,\mathrm{g/cm^{-2}}$ with a step size of $200\,\mathrm{g/cm^2}$. At zenith angles $\theta > 80^\circ$, the simulations were done at slant depths, measured from the ground, starting from $50\,\mathrm{g/cm^2}$ up to $8000\,\mathrm{g/cm^2}$ with a step size of $200\,\mathrm{g/cm^2}$. Finally, a thinning algorithm [35] was selected, with a thinning level of 10^{-7}. The kinetic energy thresholds for explicity tracking particles were set to: 100 , 100 , 0.25 , $0.25\,\mathrm{MeV}$ for hadrons, muons, electrons and photons, respectively.

In this paper proton-induced showers, simulated with the code CORSIKA [36] and considering the model QGSJET 01 [37] for interactions in the atmosphere, will be treated as the main background to detecting ν showers with the surface array of the observatory.

The detector response to AIRES simulated EAS was evaluated by retaining all the real performances of the surface array [38] implemented in the Off<u>line</u> framework [29].

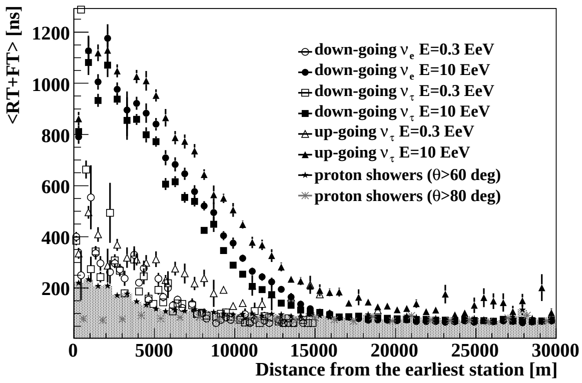

Fig. 3. *Average of the sum of rise and fall time of station signals versus distance from the earliest triggering station. Quasi-horizontal up-going ν_τ-induced showers, down-going ν_e-induced showers and down-going ν_τ-induced showers at $0.3\,\mathrm{EeV}$ and $10\,\mathrm{EeV}$, compared to inclined hadronic showers ($\theta > 60^\circ$ and $\theta > 80^\circ$) are shown.*

IV. Identifying and discriminating ν-induced showers

Hadronic showers develop after few atmospheric depths and only high-energy muons can survive to the ground. As a result, the detected showers have thin and flat fronts which lead to short and fast signals (duration $\sim 150\,\mathrm{ns}$). In young ν-induced showers a significant electromagnetic component is, instead, present at the ground as well. The shower fronts,

[1]The inelasticity is defined as the fraction of energy which the hadronic component acquires at the interaction vertex.

therefore, are curved and thick, and broad signals (duration $\lesssim 1000\,\mathrm{ns}$) are expected to be detected [39]. On the ground an early bulk of particles (electromagnetic component) is expected to trigger the earliest stations of a ν-footprint as broad signals while, later along the footprint, narrower signals are expected (asymmetric signal duration). The attenuation in the atmosphere affects also the topology of the footprints such that a "broader" structure is present in the earliest regions (asymmetric footprint structure). In ordinary hadronic showers no difference in signal duration and asymmetry in the footprints can be seen. In particular, asymmetry in the signal rise and fall times, already presented in Ref. [40], can be clearly seen in simulations of ν-induced showers (Fig. 3). The signal for ν-showers is broader around the position of the maximum of the shower development. At energies below $3\,\mathrm{EeV}$ broader signals can be observed in the two earliest triggering stations, while above $10\,\mathrm{EeV}$, broader signals can be also observed in later stations since the complete ground shower development can be detected at the ground.

The first step towards the identification of ν-events is the discrimination between young and old showers. The topology of footprints and the evolution of the station signals are the basic ingredients. Elongated footprints indicate inclined showers. A principal component analysis was used to evaluate the length (L) over the width (W) of patterns on the ground. The positions of the stations are weighted by their signals. The elongation of a footprint is defined as L/W [19]. A large value for the L/W of a footprint is not enough to estabilish whether the event, which has produced it, is inclined. Low-energy events (below $1\,\mathrm{EeV}$), expected to have low multiplicity of stations, can still have quite large L/W since the transversal development is not enough to trigger further stations. The additional parameter which was taken into account is the so-called mean apparent velocity of a shower on the ground, $\langle V\rangle$. The mean apparent velocity is defined by averaging the apparent velocity between couples of stations, defined as

$$v_{ij} = \frac{d_{ij}}{\Delta t_{ij}} \quad (3)$$

where d_{ij} is the distance between the couples, projected onto the direction defined by the length of the footprint, and Δt_{ij} the difference in their signal start times [19]. The mean apparent velocity is expected to be compatible with the speed of light for quasi-horizontal showers, within its statistical error $\sigma_{\langle V\rangle}$. The determination of $\langle V\rangle$ is strictly related to the goodness of the principal component analysis. Wider footprints, typical for more energetic showers or less inclined showers, might produce large uncertainties in the estimate of the direction of footprint length and width.

Young showers are expected to trigger detector stations with broad signals. Local ToT trigger signals are clearly broad signals (Sec. II) and counting them can help in identifying young showers. However, double muon or high energetic single-muon signals may affect the set of selected ToT stations. To strengthen the ToT condition, signals triggering for at least $375\,\mathrm{ns}$ (equivalent to 15 time bins) were retained. In

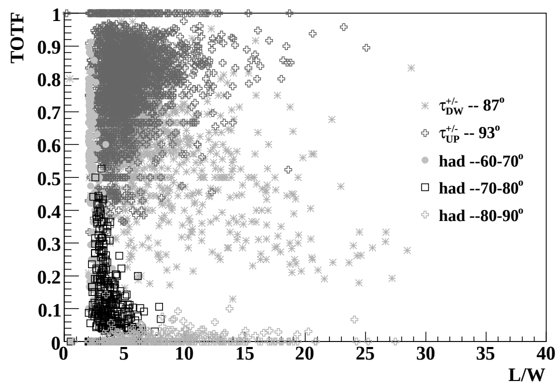

Fig. 4. *Length over width (L/W) versus fraction of ToT stations, $TOTF$.*

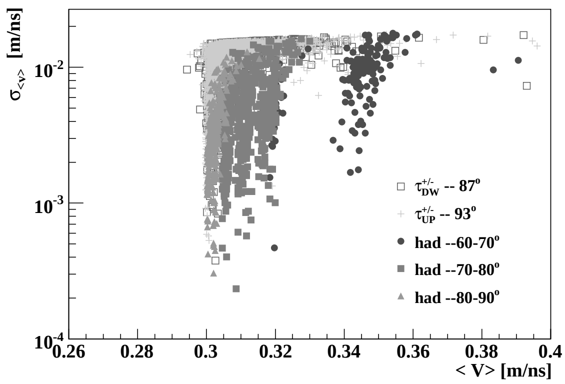

Fig. 5. *Mean apparent velocity, $\langle V\rangle$, versus its statistical uncertainty, $\sigma_{\langle V\rangle}$.*

addition, the ratio of integrated signals over their peak height was required to be larger than 1.4. The number of such ToTs over the total number of triggering stations is called $TOTF$. A similar parameter was also used in Ref. [19]. Compact configurations of selected ToTs complete the expected features of young ν-shower footprints.

A final criteria for the identification is the observation of the average rise time, $\langle RT_2\rangle$, and the average fall time, $\langle FT_2\rangle$, calculated for the 2 earliest triggered stations.

Several distributions for the parameters described above can be drawn to show the differences between proton-induced showers and ν-induced showers. In Fig. 4–6 example of distributions for showers induced by CC ν-interactions are shown. In Fig. 4, it can be observed that the fraction of young stations for hadronic showers decreases by increasing the zenith angle (the electromagnetic component is attenuated). For tau lepton showers, one expects that most of the stations have broad ToT signals, according to the definition given previously in this section, along with elongated footprints. In Fig. 5, the apparent velocity depends clearly on the zenith angle of the shower (in hadronic simulations), and, for quasi-horizontal showers with zenith angle between $85°$ and $95°$, it is tightly concentrated around the speed of light (range 0.30÷0.32 m/ns) with uncertainty below $0.02\,\mathrm{m/ns}$. In Fig. 6, the separation of $\langle RT_2\rangle$ and $\langle FT_2\rangle$ in ν-showers and proton

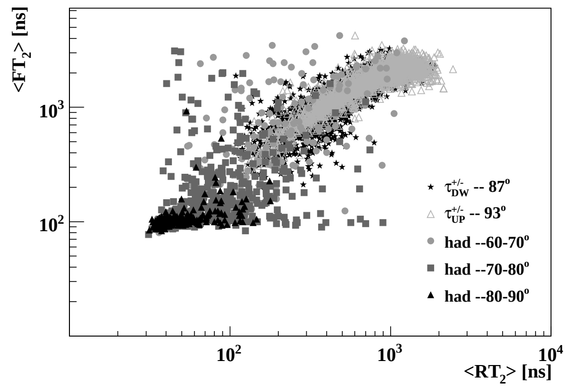

Fig. 6. *The average rise time $\langle FT\rangle_2$ as a function of the average fall time, $\langle FT\rangle_2$ calculated for the two earliest triggered stations.*

showers is more enhanced in the region where the average rise time is larger than about $80\,\mathrm{ns}$ and the average fall time is larger than $200\,\mathrm{ns}$. These values can be also produced by hadronic showers with $\theta < 70°$ but in this case the average apparent velocity is expected to be larger than the speed of light and concentrated around $0.35\,\mathrm{m/ns}$. Thus, discrimination of ν-showers from hadronic events is still possible at lower zenith angles.

In order to evaluate the best set of cuts to identify ν-showers, the program GARCON [41] was used. The six-parameter phase space $\vec{x} \equiv \{TOTF, L/W, \langle V\rangle, \sigma_{\langle V\rangle}, \langle RT_2\rangle, \langle FT_2\rangle\}$ was used to maximize the functional $F[S(\vec{x}^{cut}), B(\vec{x}^{cut})] = S(\vec{x}^{cut})/\sqrt{S(\vec{x}^{cut}) + B(\vec{x}^{cut})}$, where $S(\vec{x}^{cut})$ is the number of signal events (ν showers) passing the cuts and $B(\vec{x}^{cut})$ the number of remaining background events (proton-induced showers) surviving the cuts.

The neutrino identification efficiency, $T_{eff}(E_i, \theta, h)$, is defined as the number of ν events triggering the detector and passing the cuts (N_{cut}) over the total number of simulated AIRES showers (N_{AIRES}). The efficiency was calculated for fixed zenith angle and energy of injected particles. An example of efficiency for down-going τ-induced showers at $87°$ is shown in Fig. 7.

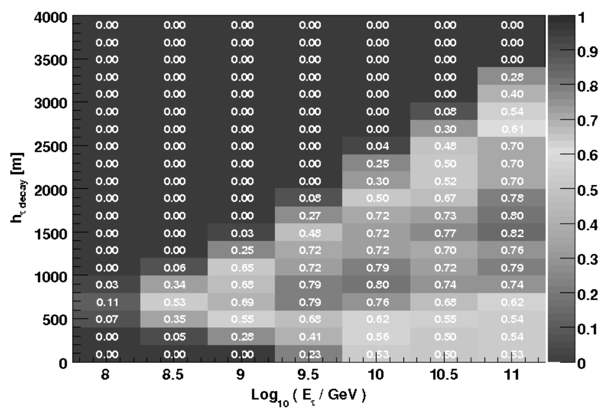

Fig. 7. *Identification efficiency for CC ν_τ-induced showers at the surface array of the Pierre Auger Observatory. Showers with 4 or more triggering stations (4-fold events) are considered.*

TABLE I

TOTAL EXPECTED EVENT RATES (CC+NC) IN (YR^{-1}) FOR THE SURFACE ARRAY OF THE PIERRE AUGER OBSERVATORY. THE VALUES ARE CALCULATED WITH A DIGITAL ELEVATION MAP AND THE ν CROSS-SECTION MODEL GRV98LO [4]. THE PRECISION ON THE LISTED VALUES IS ABOUT 4%

	WB (yr^{-1})	GZK (yr^{-1})	TD (yr^{-1})
ν_τ^{up}	0.294	0.485	2.620
ν_τ^{dw}	0.064	0.119	0.780
ν_e	0.079	0.150	0.977

V. EXPECTED EVENT RATES

The total observable rates (number of expected events) were calculated according to

$$N = \Delta T \times \int_{E_{th}}^{E_{max}} A(E_\nu) \times \Phi(E_\nu) \times dE, \qquad (4)$$

where $\Phi(E_\nu)$ is the isotropic ν-flux, ΔT the observation time and $A(E_\nu)$ the acceptance for a given initial neutrino energy, E_ν. The acceptance was calculated with the following equation

$$A(E_\nu) = N_{gen}^{-1} \times \sum_k \sum_{i=1}^{N_k} P_i(E_\nu, E_k, \theta) \times T_{eff,k}(E_k, \theta, h) \times A_i(\theta) \times \Delta\Omega, \qquad (5)$$

where N_{gen} is the number of generated neutrino events, N_k is the number of particles of type k (leptons/hadrons for CC/NC reactions) with energy E_k larger than the threshold energy of the detector (E_{th}) and for which the decay vertex positions are above the ground and inside the detector volume, $P(E_\nu, E_k, \theta)$ is the probability that a neutrino with energy E_ν and crossing the distance ΔL would produce a particle with an energy E_k (this probability was used as "weight" of the event), $A_j(\theta)$ is the cross-sectional area of the detector volume seen by the neutrino, $\Delta\Omega$ is the space angle. At high energies the effect of the mountains on the acceptance calculations is important for ν_τ-induced showers. The enhancement of the event rate for down-going ν_τ-induced showers is about 130% and for up-going ν_τ-induced showers is about 19% [26, 42]. In Tab. I the rates (number of events per year), for different injected ν-fluxes are listed. The rates labeled with "WB" are obtained for the Waxman-Bahcall bound [43], $\Phi(E_{\nu_\tau + \bar{\nu}_\tau}) = 1 \times 10^{-8} E^{-2}$ (GeV s^{-1} cm^{-2} sr^{-1}). Other rates are calculated for the GZK flux [44] and Topological Defects (TD) flux [45].

VI. SUMMARY

A complete MC simulation chain to study the possibility of detecting up- and down-going ν-induced showers with the surface array of the Pierre Auger Observatory has been presented. A more detailed study of background from deep gamma and muon showers (e.g. [46]) needs to be performed in order to predict their effective contribution to the total background.

REFERENCES

[1] J. K. Becker, High-energy neutrinos in the context of multimessenger physics, Phys. Rept. **458** (2008) 173–246.
[2] R. Gandhi, C. Quigg, M. H. Reno, I. Sarcevic, Neutrino interactions at ultrahigh energies, Phys. Rev. **D58** (1998) 093009.
[3] N. Armesto, C. Merino, G. Parente, E. Zas, Small-x Physics and the Detection of UHE Neutrinos, arXiv: hep-ph/0805.2247 (2008).
[4] M. Gluck, E. Reya, A. Vogt, Dynamical parton distributions revisited, Eur. Phys. J. **C5** (1998) 461–470.
[5] K. Mannheim, R. J. Protheroe, J. P. Rachen, On the cosmic ray bound for models of extragalactic neutrino production, Phys. Rev. **D63** (2001) 023003.
[6] SNO Collanoration [Q. R. Ahmad et al.], Direct evidence for neutrino flavor transformation from neutral-current interactions in the Sudbury Neutrino Observatory, Phys. Rev. Lett. **89** (2002) 011301.
[7] Super-Kamiokande Collaboration [Y. Fukuda et al.], Evidence for oscillation of atmospheric neutrinos, Phys. Rev. Lett. **81** (1998) 1562–1567.
[8] J. G. Learned, S. Pakvasa, Detecting tau-neutrino oscillations at PeV energies, Astropart. Phys. **3** (1995) 267–274.
[9] H. Athar, M. Jezabek, O. Yasuda, Effects of neutrino mixing on high-energy cosmic neutrino flux, Phys. Rev. **D62** (2000) 103007.
[10] J. F. Beacom, N. F. Bell, D. Hooper, S. Pakvasa, T. J. Weiler, Decay of high-energy astrophysical neutrinos, Phys. Rev. Lett. **90** (2003) 181301.
[11] Y. Farzan, A. Y. Smirnov, Leptonic unitarity triangle and CP-violation, Phys. Rev. **D65** (2002) 113001.
[12] G. Jungman, M. Kamionkowski, K. Griest, Supersymmetric dark matter, Phys. Rept. **267** (1996) 195–373.
[13] V. S. Berezinsky, G. T. Zatsepin, Cosmic rays at ultrahigh-energies (neutrino?), Phys. Lett. B **28** (1969) 423.
[14] Pierre Auger Collaboration [J. Abraham et al.], Properties and performance of the prototype instrument for the Pierre Auger Observatory, Nucl. Instrum. Meth. **A523** (2004) 50–95.
[15] K. S. Capelle, J. W. Cronin, G. Parente, E. Zas, On the detection of ultra high energy neutrinos with the Auger Observatory, Astropart. Phys. **8** (1998) 321–328.
[16] X. Bertou, P. Billoir, O. Deligny, C. Lachaud, A. Letessier-Selvon, Tau neutrinos in the Auger observatory: A new window to UHECR sources, Astropart. Phys. **17** (2002) 183–193.
[17] C. Aramo, et al., Earth-skimming UHE Tau Neutrinos at the Fluorescence Detector of Pierre Auger Observatory, Astropart. Phys. **23** (2005) 65–77.
[18] G. Miele, S. Pastor, O. Pisanti, The aperture for UHE tau neutrinos of the Auger fluorescence detector using a Digital Elevation Map, Phys. Lett. **B634** (2006) 137–142.
[19] Pierre Auger Collaboration [J. Abraham et al.], Upper Limit on the Diffuse Flux of Ultrahigh Energy Tau Neutrinos from the Pierre Auger Observatory, Phys. Rev. Lett. **100** (2008) 211101.
[20] A. Letessier-Selvon, Establishing the GZK cutoff with ultra high energy tau neutrinos, AIP Conf. Proc. **566** (2001) 157–171.
[21] D. Fargion, Discovering ultra high energy neutrinos by horizontal and upward tau air-showers: First evidences in terrestrial gamma flashes, Astrophys. J. **570** (2002) 909–925.
[22] J. L. Feng, P. Fisher, F. Wilczek, T. M. Yu, Observability of earth-skimming ultra-high energy neutrinos, Phys. Rev. Lett. **88** (2002) 161102.
[23] E. Zas, Neutrino detection with inclined air showers, New Journal of Physics **7** (2005) 130.
[24] P. Billoir, O. Blanch Bigas, The Pierre Auger Observatory and neutrinos, Nucl. Phys. Proc. Suppl. **168** (2007) 225–231.
[25] O. Blanch Bigas, Limits to the diffuse flux of UHE tau neutrinos at EeV energies from the Pierre Auger Observatory, arXiv: astro-ph/0706.1658 (2007).
[26] D. Gora, M. Roth, A. Tamburro, A MC approach to simulate up- and down-going neutrino showers including local topographic conditions, Astropart. Phys. **26** (2007) 402–413.
[27] O. Blanch Bigas, O. Deligny, K. Payet, V. Van Elewyck, UHE tau neutrino flux regeneration while skimming the Earth, Phys. Rev. **D78** (2008) 063002.
[28] X. Bertou, et al., Calibration of the surface array of the Pierre Auger Observatory, Nucl. Instrum. Meth. **A568** (2006) 839–846.
[29] S. Argiro, et al., The Offline Software Framework of the Pierre Auger Observatory, Nucl. Instrum. Meth. **A580** (2007) 1485–1496.
[30] S. I. Dutta, Y. Huang, M. H. Reno, Tau neutrino propagation and tau energy loss, Phys. Rev. **D72** (2005) 013005.
[31] Consortium for Spatial Information (CGIAR-CSI). URL `http://srtm.csi.cgiar.org/`
[32] T. Sjostrand, S. Mrenna, P. Skands, PYTHIA 6.4 physics and manual, JHEP **05** (2006) 026.
[33] S. Jadach, Z. Was, R. Decker, J. H. Kuhn, The tau decay library TAUOLA: Version 2.4, Comput. Phys. Commun. **76** (1993) 361–380.
[34] AIRES web-site. URL `http://www.fisica.unlp.edu.ar/auger/aires/`
[35] A. M. Hillas, Shower simulation: Lessons from MOCCA, Nucl. Phys. Proc. Suppl. **52B** (1997) 29–42.
[36] D. Heck, G. Schatz, T. Thouw, J. Knapp, J. N. Capdevielle, CORSIKA: A Monte Carlo code to simulate extensive air showers, FZKA-6019.
[37] N. N. Kalmykov, S. S. Ostapchenko, A. I. Pavlov, Quark-gluon string model and EAS simulation problems at ultra-high energies, Nucl. Phys. Proc. Suppl. **52B** (1997) 17–28.
[38] P. L. Ghia, Testing the surface detector simulation for the Pierre Auger Observatory, arXiv: astro-ph/0706.1212 (2007).
[39] P. Billoir, O. Blanch Bigas, The Pierre Auger Observatory and ultra high energy neutrinos, Prepared for 3rd International Workshop on NO-VE: Neutrino Oscillations in Venice: 50 Years after the Neutrino Experimental Discovery, Venice, Italy, 7-10 Feb 2006.
[40] J. Alvarez-Muniz [Auger Collaboration], The sensitivity of the surface detector of the Pierre Auger Observatory to UHE neutrinos, in: Proc. 30th ICRC, Merida, Mexico, 2007.
[41] S. Abdullin, et al., GARCON: Genetic algorithm for rectangular cuts optimization. User's manual for version 2.0, arXiv: hep-ph/0605143.
[42] D. Gora, M. Roth, A. Tamburro, A MC simulation of neutrino showers and their detection with the Pierre Auger Observatory, in: Proc. 30th ICRC, Merida, Mexico.
[43] E. Waxman, J. N. Bahcall, High energy neutrinos from astrophysical sources: An upper bound, Phys. Rev. **D59** (1999) 023002.
[44] T. Stanev, D. Seckel, R. Engel, Propagation of ultra-high energy protons in regular extragalactic magnetic fields, Phys. Rev. **D68** (2003) 103004.
[45] P. Bhattacharjee, Cosmic topological defects, highest energy cosmic rays, and the baryon asymmetry of the universe, Phys. Rev. Lett. **81** (1998) 260–263.
[46] O. Tascau, K. H. Kampert, M. Risse, R. Engel, Investigation of backgrounds for horizontal neutrino showers at ultra-high energy, in: Proc. 30th ICRC, Merida, Mexico, 2007.